Anti-Oxidizing Air-Stable Perovskite Solar Cells Using Lithium-Ion Endohedral Fullerene ($Li^+@C_{60}$) as Dopant

Il Jeon,[†,⊥] Hiroshi Ueno,[‡,⊥] Seungju Seo,[†] Kerttu Aitola,[+] Ryosuke Nishikubo,[§] Akinori Saeki,[§] Hiroshi Okada,[†] Gerrit Boschloo,[+] Shigeo Maruyama,[†] Yutaka Matsuo*[†,‡]

†Department of Mechanical Engineering, School of Engineering, The University of Tokyo, Bunkyo, Tokyo 113-8565, Japan

‡School of Chemistry, Northeast Normal University, Changchun, Jilin 130024, P. R. China

+Department of Chemistry – Ångström Laboratory Physical Chemistry Uppsala University, 75120 Uppsala, Sweden

§Department of Applied Chemistry, Graduate School of Engineering, Osaka University, Osaka 565-0871, Japan

Supporting Information Placeholder

ABSTRACT: In this communication, we report use of $[Li^+@C_{60}]TFSI^-$ as a dopant for spiro-MeOTAD in lead halide perovskite solar cells, which exhibited air stability nearly 10-fold that of conventional devices using Li^+TFSI^-. Such high stability is attributed to the hydrophobic nature of $[Li^+@C_{60}]TFSI^-$ repelling moisture and absorbing intruding oxygen, thereby protecting the perovskite device from degradation. Furthermore, $[Li^+@C_{60}]TFSI^-$ could oxidize spiro-MeOTAD without the need for oxygen. The encapsulated devices exhibited outstanding air stability for more than 1000 h while illuminated under ambient conditions.

Lead halide perovskite solar cells (PSCs) are promising solar energy sources that have received considerable attention in recent years.[1] Their certified power conversion efficiencies (PCEs) now exceed 20%.[2] However, the low stability of PSCs has been their serious drawback, one that is in dire need of resolution.[3] It has been found that light, oxygen, and water results in degradation of the perovskite layer.[4] In particular, dopants used in the hole-transporting material (HTM) 2,2′,7,7′-tetrakis(*N,N*-di-*p*-methoxyphenylamine)-9,9′-spirobi-fluorene (spiro-MeOTAD) are thought to cause low stability, due to their hygroscopic nature.[5] Replacement of liquid electrolyte with spiro-MeOTAD was a breakthrough in the initial stage of PSC development,[6] improving PCE substantially.[7] However, because spiro-MeOTAD intrinsically has low mobility, a *p*-type dopant, lithium bis(trifluoromethanesulfonyl)imide (Li^+TFSI^-) must be present to improve its conductivity.[8] Li^+TFSI^- does not directly oxidize spiro-MeOTAD; instead, it promotes the oxidation of spiro-MeOTAD by oxygen in the presence of light or thermal excitation.[8a,8b] Because doping spiro-MeOTAD with Li^+TFSI^- requires oxygen, it is difficult to control the spiro-MeOTAD oxidation; the formation of oxidized spiro-MeOTAD has been shown to be reversible during device operation depending on ambient conditions and the sweep direction in current density−voltage ($J-V$) measurement. In addition, a number of factors, including the lithium ion concentration and oxygen, increase the amount of oxidized spiro-MeOTAD.[9] Such uncontrolled oxidization of spiro-MeOTAD leads to inconsistency and instability of PSCs.[10]

In this study, lithium-ion-containing [60]fullerene trifluoromethanesulfonylimide salt ($[Li^+@C_{60}]TFSI^-$) was used in PSCs instead of Li^+TFSI^- as a solution to the aforementioned problems.[11] The encapsulation of Li^+ using the fullerene cage changed the hydrophilic alkali salt to a hydrophobic species. Additionally, spiro-MeOTAD mixed with $[Li^+@C_{60}]TFSI^-$ instantly produced the spiro-MeOTAD $^{\bullet+}TFSI^-$ salt and neutral $Li^+@C_{60}^{\bullet-}$ (= $Li@C_{60}$) by electron transfer from spiro-MeOTAD to $Li^+@C_{60}$. Spiro-MeOTAD$^{\bullet+}TFSI^-$ required no chemical additives or oxidation, because it was technically pre-oxidized spiro-MeOTAD.[12] While spiro-MeOTAD$^{\bullet+}TFSI^-$ functioned as an effective HTM, $Li^+@C_{60}^{\bullet-}$ functioned as an antioxidant, reacting with intruding oxygen. By preventing unnecessary oxidation in the device system, $[Li^+@C_{60}]TFSI^-$ devices achieved stability approximately 7-fold that of conventional Li^+TFSI^- devices in $CH_3NH_3PbI_3$-based PSCs, and 10-fold in a more stable mixed ion lead halide PSCs. Consequently, the passivated PSCs showed no decrease in PCE for more than 1000 h while being continuously illuminated under ambient conditions.

UV-vis-NIR absorption titration was used to investigate the electronic interaction between spiro-MeOTAD and $[Li^+@C_{60}]TFSI^-$. A solution of $Li^+@C_{60}TFSI^-$ was slowly added to a spiro-MeOTAD solution, and the spectra of spiro-MeOTAD were acquired in the presence of varying concentrations of $[Li^+@C_{60}]TFSI^-$. As shown in Figure 1a, the addition of $[Li^+@C_{60}]TFSI^-$ (Figure S1a) to spiro-MeOTAD solution (Figure S1b) caused characteristic absorptions to appear at around 500 nm and 1035 nm, which we assigned to oxidized spiro-MeOTAD$^{\bullet+}TFSI^-$[12] and reduced $Li^+@C_{60}^{\bullet-}$,[11c] respectively. These peaks can be seen more clearly in the magnified inset of Figure 1a. Spiro-MeOTAD has a strong peak at 390 nm, while oxidized spiro-MeOTAD has an additional small peak at around 500 nm (Figure S2a).[13] Moreover, the sharp peak at 1035 nm indicates the formation of neutral $Li^+@C_{60}^{\bullet-}$ (Figure S2b).[11c] Comparison with the simulated spectrum of a mixture of $[Li^+@C_{60}]TFSI^-$ and spiro-MeOTAD without electronic interaction (Figure 1b) indicates that $[Li^+@C_{60}]TFSI^-$ electronically interacted with spiro-MeOTAD to produce spiro-MeOTAD$^{\bullet+}TFSI^-$ and $Li^+@C_{60}^{\bullet-}$.

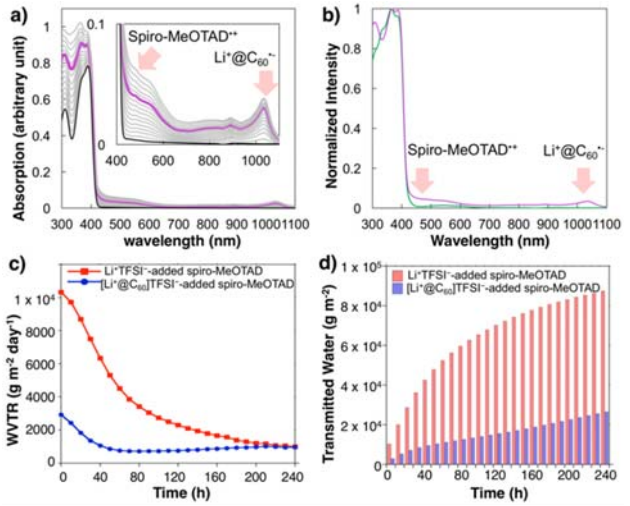

Figure 1. (a) UV-vis-NIR absorption titration of spiro-MeOTAD (8.7×10^{-6} M) in the presence of $[Li^+@C_{60}]TFSI^-$ (from 0 to 1.5 equiv) in chlorobenzene. (b) The measured spectrum of spiro-MeOTAD/$[Li^+@C_{60}]TFSI^-$ = 1:1 (purple line) compared with the simulated spectrum of spiro-MeOTAD/$[Li^+@C_{60}]TFSI^-$ = 1:1 without electronic interaction (green line). (c) WVTR change of Li^+TFSI^--added spiro-MeOTAD (red square line) and $[Li^+@C_{60}]TFSI^-$-added spiro-MeOTAD (blue circle line) over time. (d) Accumulative bar graph showing the total transmitted water through Li^+TFSI^--added spiro-MeOTAD (red bars) and $[Li^+@C_{60}]TFSI^-$-added spiro-MeOTAD (blue bars) over time.

Photoelectron yield spectroscopy was used to determine the effect of spiro-MeOTAD$^{\bullet+}TFSI^-$ formation on the energy level of HTM. Oxidizing spiro-MeOTAD introduces a hole in the highest occupied molecular orbital of spiro-MeOTAD, shifting the Fermi level downward.[10b,12-14] The addition of Li^+TFSI^- decreased the Fermi level of spiro-MeOTAD from –5.05 eV to –5.35 eV, while the addition of $[Li^+@C_{60}]TFSI^-$ lowered the Fermi level to –5.25 eV, confirming the oxidation (Figure S3).

It has been well documented that exclusion of oxygen[15] and moisture[3a,16] can significantly improve the stability of PCSs. Therefore, we assessed the hydrophilicity and barrier ability of spiro-MeOTAD films containing $[Li^+@C_{60}]TFSI^-$. Water contact angle measurements showed that the $[Li^+@C_{60}]TFSI^-$-containing spiro-MeOTAD film was more hydrophobic than a conventional Li^+TFSI^--containing film (Figure S4). This indicates that fullerene encapsulation subdues the hydrophilicity of Li^+. Next, we measured the water vapor transmittance rate (WVTR) and oxygen transmittance rate (OTR), which can quantify the hydrophobicity and antioxidant activity of the new dopant, respectively. Although both of the Li^+TFSI^--added and $[Li^+@C_{60}]TFSI^-$-added spiro-MeOTAD films showed the similar WVTR values, the $[Li^+@C_{60}]TFSI^-$-added spiro-MeOTAD film exhibited a much lower WVTR value during the initial stage. This corroborates the hydrophobicity of the $[Li^+@C_{60}]TFSI^-$-added spiro-MeOTAD film, because the initial WVTR values indicate the amount of adsorbed moisture to the films (Figure 1c). This results in more water being percolated through the Li^+TFSI^--added spiro-MeOTAD film according to the accumulative transmitted water data (Figure 1d). Contrary to the WVTR data, the OTR data reveals that $[Li^+@C_{60}]TFSI^-$-added spiro-MeOTAD film functions as a superior oxygen barrier compared with the conventional film (Figure S5). We attribute this to the antioxidant activity induced by the fullerene species. Lastly, the UV-vis absorption spectra of those films on methylammonium lead iodide ($MAPbI_3$) films were measured in air continuously under 1 sun (Figure S6). The time-course data confirm that the $[Li^+@C_{60}]TFSI^-$-containing spiro-MeOTAD film indeed maintains its PCE for the longest duration.

PSCs were fabricated using $[Li^+@C_{60}]TFSI^-$ as a dopant (Figure 2a). It is known that devices with spiro-MeOTAD show considerable electrode polarization and that addition of 4-*tert* butylpyridine (*t*-BP) decreases the *J*–*V* hysteresis of the devices.[17] We added *t*-BP to the spiro-MeOTAD and $[Li^+@C_{60}]TFSI^-$ mixture for this reason and also to inhibit complexation.[18] The photovoltaic performance of the devices is shown in Table 1. $MAPbI_3$-based PSCs gave a PCE of 13.1% using $[Li^+@C_{60}]TFSI^-$ and 17.0% using the conventional Li^+TFSI^- (Figure 2b; Figure S7 and S8). Despite the lower PCE, the PSCs with $[Li^+@C_{60}]TFSI^-$ displayed much longer stability with an extremely long light-soaking time to reach the maximum PCE and then slowly decreasing, again, over a long time (Figure 2c). This meant that the photooxidation of spiro-MeOTAD and perovskite layer was being hindered by antioxidation.[8b,12,19] The lower PCE of $[Li^+@C_{60}]TFSI^-$-used PSCs came from the lower open circuit voltage (V_{OC}) and fill factor (FF), which could be a result of the degradation of $MAPbI_3$ in air during the long light-soaking time. We incorporated formamidinuim (FA) and methylammonium (MA) mixed $(FAPbI_3)_{0.85}(MAPbBr_3)_{0.15}$-based PSCs, which is more stable than $MAPbI_3$ due to more compact cubic crystal structure.[1c] A higher PCE of 16.8% was achieved using $[Li^+@C_{60}]TFSI^-$ (Figure 2b) and such improvement can be attributed to higher V_{OC} and FF, coming from much reduced degradation of the perovskite active layer. By calculating the time from the maximum PCEs, the PSCs with $[Li^+@C_{60}]TFSI^-$ showed stability approximately 10-fold that of the reference PSCs with Li^+TFSI^- (Figure 2d).

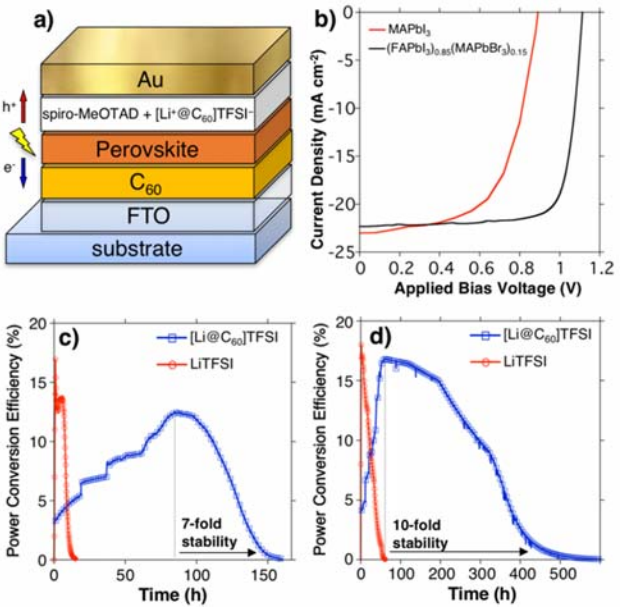

Figure 2. (a) Illustration of the PSCs with $[Li^+@C_{60}]TFSI^-$. (b) Optimum *J*–*V* curves of $MAPbI_3$- and $(FAPbI_3)_{0.85}(MAPbBr_3)_{0.15}$-PSCs using $[Li^+@C_{60}]TFSI^-$ under 1 sun. Stability data of (c) the $MAPbI_3$-PSCs and (d) the $(FAPbI_3)_{0.85}(MAPbBr_3)_{0.15}$-PSCs with $[Li^+@C_{60}]TFSI^-$ and those with Li^+TFSI^-, the test condition was that the devices were unencapsulated in air under constant illumination.

Table 1. Photovoltaic parameters of the conventional PSCs with Li^+TFSI^- and PSCs with $[Li^+@C_{60}]TFSI^-$ (Table S1).

Perovskite	Dopant	J_{SC} (mA/cm^2)	V_{OC} (V)	FF	PCE (%)
$MAPbI_3$	Li^+TFSI^-	22.2	1.07	0.72	17.0
	$[Li^+@C_{60}]TFSI^-$	23.0	0.89	0.63	13.1
$(FAPbI_3)_{0.85}$ $(MAPbBr_3)_{0.15}$	Li^+TFSI^-	22.2	1.11	0.75	18.5
	$[Li^+@C_{60}]TFSI^-$	22.9	1.01	0.72	16.8

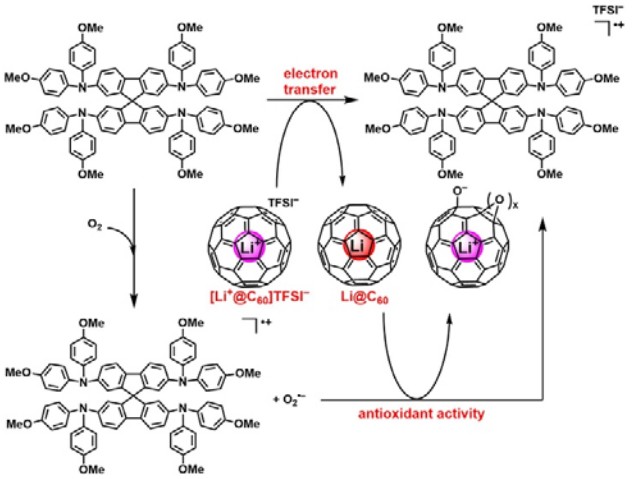

Figure 3. Schematic diagram of the proposed mechanism inside the new HTM.

This phenomenon can be understood by assessing the chemical reactions that occur inside the HTM. In the case of the reference devices, the reaction between spiro-MeOTAD and Li^+TFSI^- involves the oxidation of spiro-MeOTAD, which is fast but uncontrolled.[20] Because this reaction is reversible, excessive oxygen leads to rapid degradation of the device,[21] while a lack of oxygen can shift the equilibrium back toward neutral spiro-MeOTAD (eq. 1 and 2). This causes the momentarily high PCE to decrease rapidly from its peak (Figures 2c and 2d).

$$spiro\text{-}MeOTAD + O_2 \rightleftharpoons spiro\text{-}MeOTAD^{\cdot+}O_2^{\cdot-} \quad (1)$$

$$spiro\text{-}MeOTAD^{\cdot+}O_2^{\cdot-} + Li^+TFSI^- \rightarrow spiro\text{-}MeOTAD^{\cdot+}TFSI^- + Li_xO_y \quad (2)$$

Alternatively, the PSCs with $[Li^+@C_{60}]TFSI^-$ avoided this problem by directly generating spiro-MeOTAD$^{\bullet+}$TFSI$^-$ and $Li@C_{60}$ species that functioned as an antioxidant. Initial PCEs of around 4% in both $MAPbI_3$ and $(FAPbI_3)_{0.85}(MAPbBr_3)_{0.15}$ systems without exposure to light and oxygen, indicate the formation of a stable amount of oxidized spiro-MeOTAD (eq. 3) (Table S2, Figure S9). Increase in the concentration of $[Li^+@C_{60}]TFSI^-$ did not increase the PCE beyond 4% due to limited solubility of $[Li^+@C_{60}]TFSI^-$ (Table S3). In addition, PSCs with poly(3-hexylthiophene-2,5-diyl) (P3HT) and $[Li^+@C_{60}]TFSI^-$ resulted in a lower PCE with severe hysteresis, though Li^+TFSI^- is supposed to dope P3HT effectively (Table S4).[8e] This indicates that the generation of spiro-MeOTAD$^{\bullet+}$TFSI$^-$ by a reaction with spiro-MeOTAD is essential for $[Li^+@C_{60}]TFSI^-$ to perform in PSCs.

$$spiro\text{-}MeOTAD + [Li^+@C_{60}]TFSI^- \rightleftharpoons spiro\text{-}MeOTAD^{\cdot+}TFSI^- + [Li^+@C_{60}]^{\cdot-} \quad (3)$$

The slow increase in PCE is attributed to the generation of oxidized spiro-MeOTAD being inhibited by neutral $[Li^+@C_{60}]^{\bullet-}$ (eq. 1), which reacts with oxygen (eq. 4), as shown in Figure 3.[22] Considering the presence of the many double bonds on fullerenes, and thus the many potential oxidation sites, the PCE does not start to drop until this anti-oxidant activity is outweighed by the degradation of perovskite.

$$[Li^+@C_{60}]^{\cdot-} + O_2 \text{ or } O_2^{\cdot-} \rightarrow Li^+@C_{60}O_xO^- \text{ etc.} \quad (4)$$

We used time-resolved microwave conductivity (TRMC) to analyze hour-scale oxidation and resultant change in optoelectronics within the HTMs.[23] According to the TRMC results (Figure S10), the spiro-MeOTAD/Li^+TFSI^- film had increasing photoconductivity for about 20 h, followed by a drop indicating uncontrolled oxidation. By contrast, the spiro-MeOTAD/$[Li^+@C_{60}]TFSI^-$ films had continuously increasing photoconductivity over an extended period exceeding that of its Li^+TFSI^- counterpart. This supports our hypothesis of controlled oxidation and antioxidant activity in the spiro-MeOTAD and $[Li^+@C_{60}]TFSI^-$ HTM.

Long-term stability tests of passivated PSCs showed that the $[Li^+@C_{60}]TFSI^-$-added device exhibited no decrease in PCE even for the less stable $MAPbI_3$ system for 1000 h while continuously illuminated under ambient conditions of 30°C and 40% relative humidity (Figure S11).

In conclusion, we discovered that $[Li^+@C_{60}]TFSI^-$ can be used as an alternative to Li^+TFSI^- as a dopant for spiro-MeOTAD in PSCs. PSCs with $[Li^+@C_{60}]TFSI^-$ exhibited significantly higher stability. This long duration of stability is ascribed to the hydrophilic nature of the fullerene cage encapsulating Li^+ and the antioxidant attributes of $Li^+@C_{60}$ shown through various analyses. It should be noted that further optimization of component concentrations and film morphology could increase the PCE even higher. To our knowledge, this work is the first to demonstrate the application of a Li-containing fullerene device and successfully address the problem of perovskite solar cell stability, indicating a potentially fruitful new direction of research in the field of solar cells and fullerenes.

ASSOCIATED CONTENT

Supporting Information

This material is available free of charge via the Internet at http://pubs.acs.org.

AUTHOR INFORMATION

Corresponding Author

matsuo@photon.t.u-tokyo.ac.jp

Notes

The authors declare no competing financial interests.

⊥ These authors contributed equally.

ACKNOWLEDGMENT

I.J. thanks the Research and Education Consortium for Innovation of Advanced Integrated Science by Japan Science and Technology (JST) and Japan Society for the Promotion of Science (JSPS) Start-up Grant (17H06609) for financial support. This work was supported by JSPS KAKENHI Grant Numbers JP25107002, JP15H05760, JP16H02285 the CREST project, and IRENA Project by JST-EC DG RTD, Strategic International Collaborative Research Program, SICORP. Part of this work is based on results obtained from a project commissioned by the New Energy and Industrial Technology Development Organization (NEDO).

REFERENCES

(1) a) McGehee, M. D. *Nat. Mater.* **2014**, *13*, 845. b) Green, M. A.; Ho-Baillie, A.; Snaith, H. J. *Nat. Photonics* **2014**, *8*, 506. c) Jeon, N. J.; Noh, J. H.; Yang, W. S.; Kim, Y. C.; Ryu, S.; Seo, J.; Seok, S. I. Nature **2015**, *517*, 476. d) Lee, J.-W.; Bae, S.-H.; Hsieh, Y.-T.; De Marco, N.; Wang, M.; Sun, P.; Yang, Y. *Chem* **2017**, *3*, 290. e) Lee, J.-W.; Kim, S.-G.; Bae, S.-H.; Lee, D.-K.; Lin, O.; Yang, Y.; Park, N.-G. *Nano Lett.* **2017**, *17*, 4270.

(2) a) Li, X.; Bi, D.; Yi, C.; Decoppet, J.-D.; Luo, J.; Zakeeruddin, S. M.;

Hagfeldt, A.; Gratzel, M. *Science* **2016**, *353*, 58. b) Seo, J.; Noh, J. H.; Seok, S. Il. *Acc. Chem. Res.* **2016**, *49*, 562. c) Kim, H.; Lim, K.-G.; Lee, T.-W. *Energy Environ. Sci.* **2016**, *9*, 12. d) Lim, K.-G.; Kim, H.-B.; Jeong, J.; Kim, H.; Kim, J. Y.; Lee, T.-W. *Adv. Mater.* **2014**, *26*, 6461.
(3) a) Noh, J. H.; Im, S. H.; Heo, J. H.; Mandal, T. N.; Seok, S. Il. *Nano Lett.* **2013**, *13*, 1764. b) Ahn, N.; Kwak, K.; Jang, M. S.; Yoon, H.; Lee, B. Y.; Lee, J.; Pikhitsa, P. V; Byun, J.; Choi, M. *Nat. Commun.* **2016**, *7*, 13422. c) Yue, Y.; Salim, N. T.; Wu, Y.; Yang, X.; Islam, A.; Chen, W.; Liu, J.; Bi, E.; Xie, F.; Cai, M.; Han, L. *Adv. Mater.* **2016**, *28*, 10738. d) Guo, Y.; Sato, W.; Shoyama, K.; Halim, H.; Itabashi, Y.; Shang, R.; Nakamura, E. *J. Am. Chem. Soc.* **2017**, *139*, 9598. e)Ahn, S.; Jeong, S.-H.; Han, T.-H.; Lee, T.-W. *Adv. Opt. Mater.* **2017**, *5*, 1600512. f) Bae, S.-H.; Zhao, H.; Hsieh, Y.-T.; Zuo, L.; Marco, N. D.; Rim, Y. S.; Li, G.; Yang, Y. *Chem* **2016**, *1*, 197.
(4) a) Leijtens, T.; Eperon, G. E.; Pathak, S.; Abate, A.; Lee, M. M.; Snaith, H. J. *Nat. Commun.* **2013**, *4*, 1. b) Bryant, D.; Aristidou, N.; Pont, S.; Sanchez-Molina, I.; Chotchunangatchaval, T.; Wheeler, S.; Durrant, J. R.; Haque, S. A. *Energy Environ. Sci.* **2016**, *9*, 1655.
(5) a) Liu, J.; Wu, Y.; Qin, C.; Yang, X.; Yasuda, T.; Islam, A.; Zhang, K.; Peng, W.; Chen, W.; Han, L. *Energy Environ. Sci.* **2014**, *7*, 2963. b) Habisreutinger, S. N.; Leijtens, T.; Eperon, G. E.; Stranks, S. D.; Nicholas, R. J.; Snaith, H. J. *Nano Lett.* **2014**, *14*, 5561.
(6) a) Lee, M. M.; Teuscher, J.; Miyasaka, T.; Murakami, T. N.; Snaith, H. J. *Science* **2012**, *338*, 643. b) Kim, H.-S.; Lee, C.-R.; Im, J.-H.; Lee, K.-B.; Moehl, T.; Marchioro, A.; Moon, S.-J.; Humphry-Baker, R.; Yum, J.-H.; Moser, J. E.; Grätzel, M.; Park, N.-G. *Sci. Rep.* **2012**, *2*, 591.
(7) a) Kwon, Y. S.; Lim, J.; Song, I.; Song, I. Y.; Shin, W. S.; Moon, S.-J.; Park, T. *J. Mater. Chem.* **2012**, *22*, 8641. b) Burschka, J.; Dualeh, A.; Kessler, F.; Baranoff, E.; Cevey-Ha, N.-L.; Yi, C.; Nazeeruddin, M. K.; Grätzel, M. *J. Am. Chem. Soc.* **2011**, *133*, 18042. c) Yang, L.; Cappel, U. B.; Unger, E. L.; Karlsson, M.; Karlsson, K. M.; Gabrielsson, E.; Sun, L.; Boschloo, G.; Hagfeldt, A.; Johansson, E. M. J. *Phys. Chem. Chem. Phys.* **2012**, *14*, 779. d) Leijtens, T.; Ding, I.-K.; Giovenzana, T.; Bloking, J. T.; McGehee, M. D.; Sellinger, A. *ACS Nano* **2012**, *6*, 1455.
(8) a) Abate, A.; Leijtens, T.; Pathak, S.; Teuscher, J.; Avolio, R.; Errico, M. E.; Kirkpatrik, J.; Ball, J. M.; Docampo, P.; McPherson, I.; Snaith, H. J. *Phys. Chem. Chem. Phys.* **2013**, *15*, 2572. b) Cappel, U. B.; Daeneke, T.; Bach, U. *Nano Lett.* **2012**, *12*, 4925. Hawash, Z.; Ono, L. K.; Raga, S. R.; Lee, M. V.; Qi, Y. *Chem. Mater.* **2015**, *27*, 562. c) Yang, L.; Xu, B.; Bi, D.; Tian, H.; Boschloo, G.; Sun, L.; Hagfeldt, A.; Johansson, E. M. J. *J. Am. Chem. Soc.* **2013**, *135*, 7378. d) Kazim, S.; Nazeeruddin, M. K.; Grätzel, M.; Ahmad, S. *Angew. Chemie Int. Ed.* **2014**, *53*, 2812. e)
(9) a) Snaith, H. J.; Grätzel, M. *Appl. Phys. Lett.* **2006**, *89*, 262114. b) Xu, B.; Huang, J.; Ågren, H.; Kloo, L.; Hagfeldt, A.; Sun, L. *ChemSusChem* **2014**, *7*, 3252.
(10) a) Leijtens, T.; Lim, J.; Teuscher, J.; Park, T.; Snaith, H. J. *Adv. Mater.* **2013**, *25*, 3227. b) MacDiarmid, A. G. *Angew. Chemie Int. Ed.* **2001**, *40*, 2581.
(11) a) Aoyagi, S.; Nishibori, E.; Sawa, H.; Sugimoto, K.; Takata, M.; Miyata, Y.; Kitaura, R.; Shinohara, H.; Okada, H.; Sakai, T.; Ono, Y.; Kawachi, K.; Yokoo, K.; Ono, S.; Omote, K.; Kasama, Y.; Ishikawa, S.; Komuro, T.; Tobita, H. *Nat. Chem.* **2010**, *2*, 678. b) Okada, H.; Matsuo, Y. *Fuller. Nanotub. Car. N.* **2014**, *22*, 262. c) Ueno, H.; Aoyagi, S.; Yamazaki, Y.; Ohkubo, K.; Ikuma, N.; Okada, H.; Kato, T.; Matsuo, Y.; Fukuzumi, S.; Kokubo, K. *Chem. Sci.* **2016**, *7*, 5770. d) Matsuo, Y.; Okada, H.; Ueno, H. *Endohedral Lithium-containing Fullerenes*; Springer Singapore: Singapore, 2017.
(12) Nguyen, W. H.; Bailie, C. D.; Unger, E. L.; McGehee, M. D. *J. Am. Chem. Soc.* **2014**, *136*, 10996.
(13) Fantacci, S.; De Angelis, F.; Nazeeruddin, M. K.; Grätzel, M. *J. Phys. Chem. C* **2011**, *115*, 23126.
(14) Zhang, Y.; Zhou, H.; Seifter, J.; Ying, L.; Mikhailovsky, A.; Heeger, A. J.; Bazan, G. C.; Nguyen, T.-Q. *Adv. Mater.* **2013**, *25*, 7038.
(15) Tidwell, T. *Nat. Chem.* **2013**, *5*, 637.
(16) Tennakone, K.; Kumara, G. R. R. A.; Kottegoda, I. R. M.; Wijayantha, K. G. U. *Semicond. Sci. Technol.* **1997**, *12*, 128.
(17) Kim, H.; Jang, I.; Ahn, N.; Choi, M.; Guerrero, A.; Bisquert, J.; Park, N. *J. Phys. Chem. Lett.* **2015**, *6*, 4633.
(18) Helgeson, H. C. *J. Phys. Chem.* **1967**, *71*, 3121.
(19) a) Wang, S.; Yuan, W.; Meng, Y. S. *ACS Appl. Mater. Interfaces* **2015**, *7*, 24791. b) Tiwana, P.; Docampo, P.; Johnston, M. B.; Herz, L. M.; Snaith, H. J. *Energy Environ. Sci.* **2012**, *5*, 9566.
(20) Schölin, R.; Karlsson, M. H.; Eriksson, S. K.; Siegbahn, H.; Johansson, E. M. J.; Rensmo, H. *J. Phys. Chem. C* **2012**, *116*, 26300.
(21) Aristidou, N.; Sanchez-Molina, I.; Chotchuangchutchaval, T.; Brown, M.; Martinez, L.; Rath, T.; Haque, S. A. *Angew. Chemie Int. Ed.* **2015**, *54*, 8208.
(22) a) Reed, C. A.; Bolskar, R. D. *Chem. Rev.* **2000**, *100*, 1075. b) Creegan, K. M.; Robbins, J. L.; Robbins, W. K.; Millar, J. M.; Sherwood, R. D.; Tindall, P. J.; Cox, D. M.; McCauley, J. P.; Jones, D. R. *J. Am. Chem. Soc.* **1992**, *114*, 1103.
(23) Ishida, N.; Wakamiya, A.; Saeki, A. *ACS Photonics* **2016**, *3*, 1678.